metals

MDPI

Article

Evidence of Change in the Density of States during the Martensitic Phase Transformation of Ni-Mn-In Metamagnetic Shape Memory Alloys

Rie Y Umetsu [1,*], Xiao Xu [2], Wataru Ito [3] and Ryosuke Kainuma [2]

[1] Institute for Materials Research, Tohoku University, Sendai 980-8577, Japan
[2] Department of Materials Science, Graduate School of Engineering, Tohoku University, Sendai 980-8579, Japan; xu@material.tohoku.ac.jp (X.X.); kainuma@material.tohoku.ac.jp (R.K.)
[3] National Institute of Technology, Sendai College, Natori 981-1239, Japan; ito@sendai-nct.ac.jp
* Correspondence: rieume@imr.tohoku.ac.jp; Tel.: +81-22-215-2199

Received: 11 August 2017; Accepted: 27 September 2017; Published: 4 October 2017

Abstract: Specific heat measurements were performed at low temperatures for $Ni_{50}Mn_{50-x}In_x$ alloys to determine their Debye temperatures (θ_D) and electronic specific heat coefficients (γ). For $x \leq 15$, where the ground state is the martensite (M) phase, θ_D decreases linearly and γ increases slightly with increasing In content. For $x \geq 16.2$, where the ground state is the ferromagnetic parent (P) phase, γ increases with decreasing In content. Extrapolations of the composition dependences of θ_D and γ in both the phases suggest that these values change discontinuously during the martensitic phase transformation. The value of θ_D in the M phase is larger than that in the P phase. The behavior is in accordance with the fact that the volume of the M phase is more compressive than that of the P phase. On the other hand, γ is slightly larger in the P phase, in good agreement with the reported density of states around the Fermi energy obtained by the first-principle calculations.

Keywords: electronic specific heat coefficient; density of states; shape memory alloy; martensitic phase transformation

1. Introduction

Since a unique martensitic phase transformation in off-stoichiometric Heusler NiMnZ (Z = In, Sn, and Sb) alloys were first reported by Sutou et al. [1], NiMnIn- and NiMnSn-based alloys have attracted widespread interest as high-performance multiferroic materials. The alloys show many interesting properties, such as metamagnetic shape memory effect [2,3] inverse magnetocaloric effect [4–6], giant magnetoresistance effect [7,8], and giant magnetothermal conductivity [9]. These interesting physical properties are related to drastic changes in magnetic properties between the ferromagnetic parent (P) phase and the martensite (M) phase with weak magnetism. Such large changes of the various physical properties should be due to the change in the electronic state during the martensitic phase transformation. First-principles density-functional calculations and hard X-ray photoelectron spectroscopy (HAXPES) experiments were performed to investigate the electronic states in the P and M phases of Ni-Mn-In alloys [10]. In these calculations, composition dependence of the partial density of states (DOS) in the P phase for Ni-Mn-In was investigated using the periodic supercells, in addition to that in the M phase, where tetragonal distortion was introduced. The valence-band photoelectron spectra of the $Ni_{50}Mn_{34}In_{16}$ alloy in warming and cooling processes showed that the peak near the Fermi energy (E_F) in the P phase disappeared in the M phase temperature range, suggesting the formation of the pseudo-gap. The minority-spin Ni $3d$–e_g state has also been concluded to play an important role in stabilizing the M phase in off-stoichiometric composition [10].

Herein, we performed specific heat measurements in Ni-Mn-In alloy system to investigate the electronic specific heat coefficient (γ), which will provide information on the DOS around E_F, and the Debye temperature (θ_D). The obtained results may provide indirect information on the electronic state, in contrast to the photoelectron spectroscopy observations that provide direct information. However, it has been reported that the value of γ for $L1_0$-type NiMn alloy and related materials (i.e., PdMn and PtMn) where the existence of the pseudo-gap around E_F characterizes their unique electronic states agrees well with the value obtained by theoretical calculations [11–13]. Systematic study of the specific heat measurements in a wide composition region for Ni-Mn-In will help understand the behavior of the metamagnetic shape memory alloys in this system.

2. Experimental Procedure

$Ni_{50}Mn_{50-x}In_x$ ($0 \leq x \leq 25$) alloys were fabricated by induction melting in an Ar atmosphere. The specimens were sealed in a quartz capsule and were annealed at 1173 K for 1 day before quenching in water. The microstructure and composition were confirmed by the electron probe microanalyzer. The crystal structure was investigated by powder X-ray diffraction and transmission electron microscope observations. The related results were reported in the previous paper [14]. The magnetic measurements were carried out on a superconducting quantum interference device (SQUID; Quantum Design Ltd., San Diego, CA, USA) magnetometer. Specific heat measurements were carried out by the relaxation method using a physical properties measurement system (PPMS produced by Quantum Design Ltd., San Diego, CA, USA) at temperatures below 20 K. The absolute value of the specific heat was checked by measuring one of the standard pure Cr.

3. Results and Discussion

3.1. Magnetic Measurements

Figure 1a,b show magnetization (*M*–*H*) curves obtained at 5 K and thermomagnetization (*M*–*T*) curves obtained under a magnetic field of 10 kOe for $Ni_{50}Mn_{50-x}In_x$ alloy specimens having $x \leq 15$, respectively. Here, the ground state of the specimens is the martensite (M) phase. The specimen with $x = 0$ (NiMn) has been reported to be collinear-type antiferromagnetic with the Néel temperature higher than the martensitic transformation temperature [15]. Therefore, the magnetic state is deduced to be antiferromagnetic for low In concentrations, and the antiferromagnetic exchange interaction in the system decreases with increasing In content [16,17]. The NiMn has an $L1_0$-type tetragonal structure with lattice parameters of $a = 0.374$ and $c = 0.352$ nm, and it transforms to $B2$-type cubic one at the martensitic transformation temperature [15]. With increasing the In concentration, the crystal structure of M phase varies to 14 M and 10 M stacking monoclinic structures [14,18,19]. The straight line in the *M*–*H* curves (Figure 1a) is characteristic of the antiferromagnetic properties. The slope increases with increasing In content, and the *M*–*H* curve indicates small hysteresis at $x = 13$. In the *M*–*H* curve for $x = 15$ (inset of Figure 1a), large hysteresis is observed, and magnetization tends to saturation. This variation arises in the magnetization curves because ferromagnetic exchange interaction is introduced with increasing In content. AC magnetization measurements have suggested that the ground state for $x = 15$ is the blocking state, showing frequency dependence in both the real and imaginary parts of the susceptibility [20]. The variation of magnetic property from the antiferromagnetic state to the blocking state is also confirmed by the *M*–*T* curves for $Ni_{50}Mn_{50-x}In_x$ alloys with $x \leq 15$. In the measurements for obtaining the *M*–*T* curves, the specimens were cooled to low temperatures in zero magnetic field, and the magnetization was measured in warming process and cooling process under the same applied magnetic field. Magnetization at lower temperatures gradually increases with increasing In content, and magnetic field cooling effect is observed for $x = 10$, 13, and 15. The large magnetization change observed at ~300 K in the *M*–*T* curve for $x = 15$ (inset of Figure 1b) is due to the martensitic phase transformation, and the magnetic property at temperatures just below the transition temperature has been concluded to be paramagnetic based on Mössbauer spectroscopy [21].

These results along with previous reports on AC magnetization measurements [20], suggest that antiferromagnetic long-range ordering might have disappeared somewhere in the composition region.

M–H curves obtained at 5 K and *M–T* curves obtained under a magnetic field of 500 Oe for specimens with $x \geq 16.2$ in $Ni_{50}Mn_{50-x}In_x$ alloys are shown in Figure 2a,b, respectively. Here, the ground state of the system is the ferromagnetic parent (P) phase. That is, no martensitic transformation occurs down to low temperatures in these composition regions. The crystal structure is basically the $L2_1$-type structure. The lattice parameter has been reported to a = 0.6071 nm for the x = 25 at room temperature and to decrease linearly with increasing the Mn composition [22]. The Figure 2b shows only warming process in *M–T* curves because there is almost no magnetic field cooling effect, in contrast to that for $x \leq 15$ in Figure 1b. The saturated magnetization increases with decreasing In content from the stoichiometric composition of $Ni_{50}Mn_{25}In_{25}$ (=Ni_2MnIn). On the other hand, concentration dependence of the Curie temperature (T_C) does not show the systematic variation as is shown by saturation magnetization. Figure 2b shows that the value of T_C is ~320 K, independent of In content.

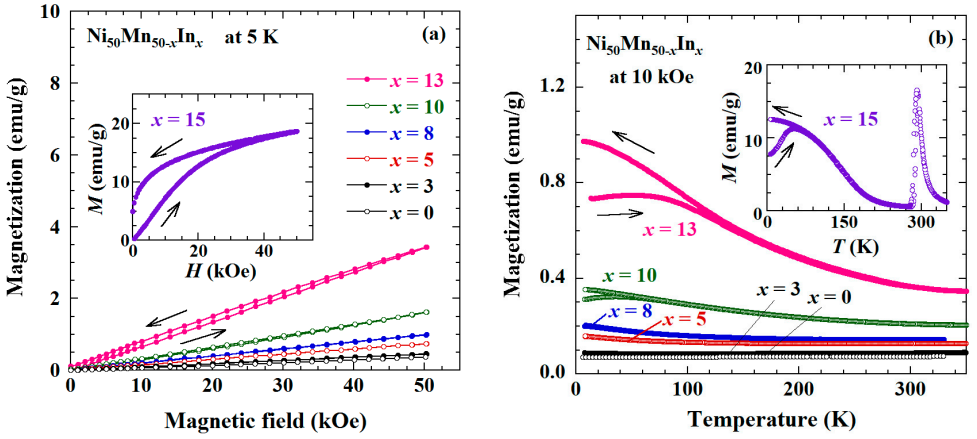

Figure 1. (**a**) Magnetization curves at 5 K and (**b**) thermomagnetization curves measured at 10 kOe for the specimens with $x \leq 15$ in $Ni_{50}Mn_{50-x}In_x$ alloys. The arrows in the figures mean applying and removing magnetic fields in (**a**), and the warming and cooling processes in (**b**). Here, the ground state of the specimens is the martensite phase. The insets are those for x = 15.

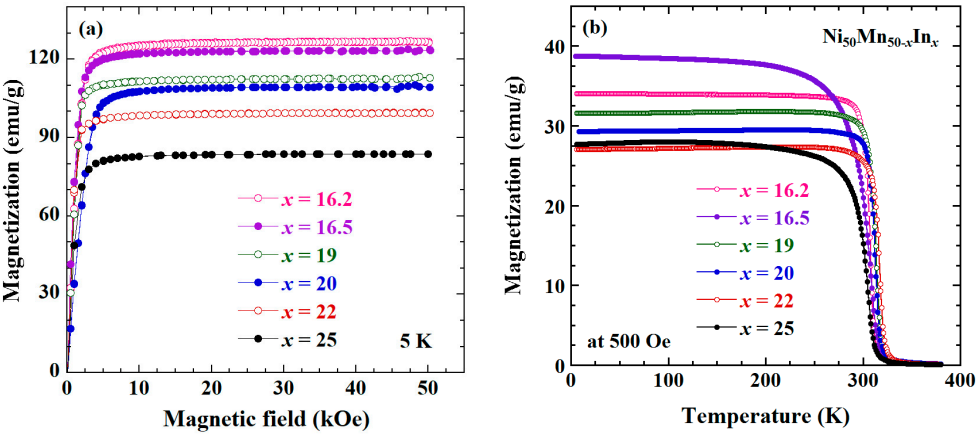

Figure 2. (**a**) Magnetization curves at 5 K and (**b**) thermomagnetization curves measured at 500 Oe in the warming process for the specimens with $x \geq 16.2$ in $Ni_{50}Mn_{50-x}In_x$ alloys. Here, the ground state of the system is the ferromagnetic parent phase and no martensitic transformation occurs down to low temperatures.

Figure 3 indicates concentration dependences of saturation magnetization (I_s) and T_C for $Ni_{50}Mn_{50-x}In_x$ alloys with $x \geq 16.2$, together with reported experimental values [22] and the theoretically calculated one for the stoichiometric composition [23]. Here, I_s is determined by linear extrapolation of the M^2 versus H/M curve to $H/M = 0$ (Arrott plot), from the data in Figure 2a. I_s increases almost linearly with decreasing In content, or in other words, with increasing Mn content. For the stoichiometric composition of $Ni_{50}Mn_{25}In_{25}$ (=Ni_2MnIn), the Ni atoms locate at the 8*c* site, and the Mn and In atoms at the 4*a* and 4*b* sites in the Wyckoff position, respectively. In the present series of the specimens, excess Mn substituted for In at the 4*b* site. Therefore, the increasing of I_s with increasing the Mn means that the magnetic moment of Mn atoms at the 4*b* site couples ferromagnetically with that of the Mn atoms at the ordinary site (4*a* site). A solid straight line is drawn, assuming that the magnitude of the magnetic moment of Mn at the 4*b* site is the same as that of Mn at the 4*a* site, and the experimental values are in good agreement with the expected line [24]. Here, the values of the magnetic moments (m) are used as $m_{Mn} = 3.719$, $m_{Ni} = 0.277$ and $m_{In} = -0.066$ μ_B, which are obtained from the first principle calculation [23]. The T_C values for all the specimens with $x \geq 16.2$ are similar (the variation is <15 K) and they are independent to the composition. This behavior suggests that the T_C is governed by the exchange interaction between Mn atoms at the 4*a* site, and the interaction by the Mn atoms at the 4*b* site does not affect the total exchange interaction in the system. This behavior of T_C was studied earlier over a wide concentration region by Miyamoto et al. [25], who reported that T_C decreases drastically with increases In concentration in $Ni_{50}Mn_{50-y}In_y$ alloys with $y > 25$. Here, excess In substituted the Mn atoms at the 4*a* site, therefore, the decrease in T_C is probably caused by the lack of Mn–Mn exchange interactions at the 4*a* site, if the magnetic moment of Mn atoms are assumed not to change.

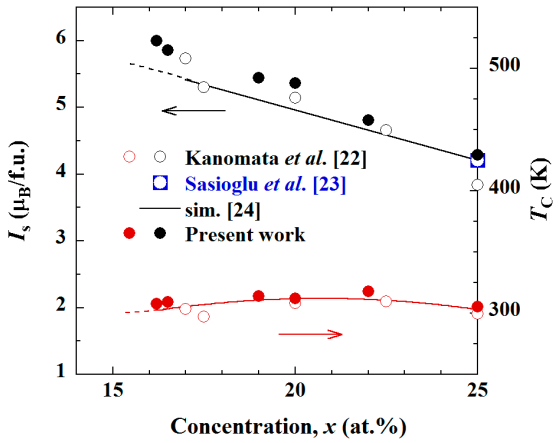

Figure 3. Concentration dependences of the spontaneous magnetization (I_s) evaluated from the magnetization curves in Figure 2a, along with reported experimental and theoretically calculated values [22,23], and of the Curie temperature (T_C) for $Ni_{50}Mn_{50-x}In_x$ alloys with $x \geq 16.2$. The solid straight line for I_s is simulated assuming that the excess Mn atoms have same magnetic moment as that of Mn at the ordinary sites and couples ferromagnetically [24]. The solid line for T_C is guide to the eye.

3.2. Specific Heat Measurements

Figure 4a,b show the relationship between specific heat (C) and temperature (T) in C/T–T^2 plots for $x \leq 15$ and $x \geq 16.2$, respectively, the insets show C–T plots for each specimen. The specific heat is generally expressed as the summation of some contributions like electronic, lattice, and magnetic contributions. When the experiments are performed at low temperatures, the magnetic excitation has little contribution to the specific heat and the other two components become dominant as follows [26]:

$$C = \gamma T + \beta T^3, \quad (1)$$

where, the first and second terms are the electronic and lattice contributions, respectively, in which γ is the electronic specific heat coefficient and β is the lattice coefficient. In the classical model, γ is thought to correspond to the total DOS. In the C/T–T^2 plot, when a linear relationship is obtained, γ and β are given by the intercept and the slope, respectively. Furthermore, θ_D is given by the relation

$$\theta_D = \sqrt[3]{12\pi^4 R/5\beta}, \quad (2)$$

where R is the gas constant [26]. As shown in Figure 4a,b, a linear relationship is obtained, and the behaviors of these coefficients in terms of composition are different in each figure (i.e., in the M phase and in the P phase). In Figure 4a, for specimens with $x \leq 15$, in which the ground state is the M phase, γ increases with increasing In content. The slope also increases, corresponding to the decrease of θ_D. On the other hand, in Figure 4b for specimens with $x \geq 16.2$, in which the ground state is the ferromagnetic P phase, γ changes slightly and slope is increased with increasing In content.

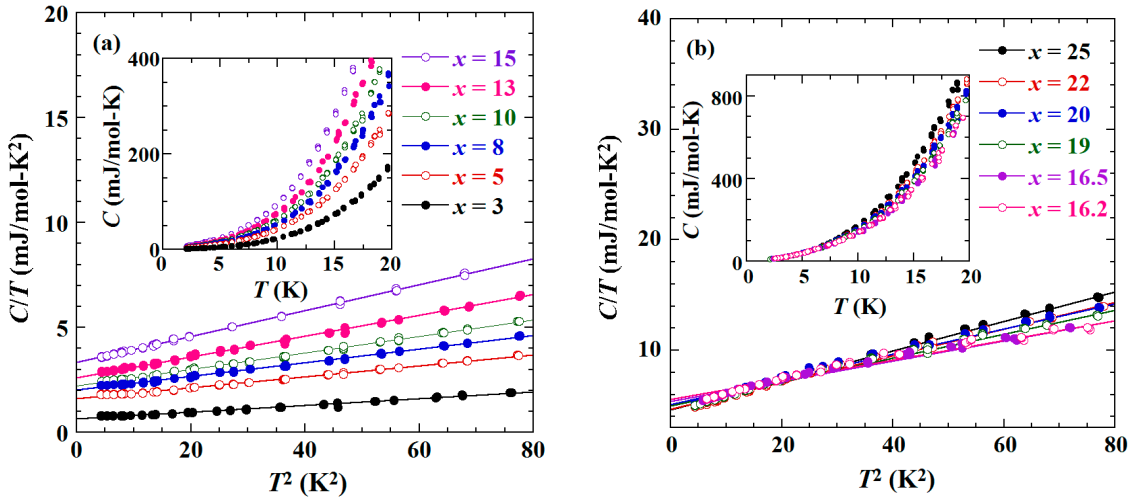

Figure 4. (**a**) C/T–T^2 plot for the specific heat (C) as a function of temperature (T) for (**a**) $x \leq 15$ and (**b**) $x \geq 16.2$ in $Ni_{50}Mn_{50-x}In_x$ alloys. Insets are C–T plots for each specimen.

Concentration dependences of γ and θ_D in $Ni_{50}Mn_{50-x}In_x$ alloys are shown in Figure 5, together with the reported values of γ = 0.31 mJ/mol·K^2 and θ_D = 422 K for x = 0 [11]. The θ_D value decreases linearly with increasing In content in the M phase region. It has been reported that the crystal structure changes continuously from $L1_0$-type tetragonal structure for x = 0 to monoclinic multi-layered stacking structure with increasing In content [18]. Magnetic property is collinear-type antiferromagnetic with high Néel temperature for x = 0 [15]. This property changes to complicated magnetic properties, in which long-range magnetic ordering is absent and blocking behavior is observed [18,21]. Since neither crystal structure nor magnetic properties change sharply with changing In content, the decrease in θ_D may be caused by the substitution effect of the heavy element In. In the M phase range, γ increases gradually with increasing In content. The electronic state of x = 0 is characterized by the formation of a clear pseud-gap around E_F and it has been reported that the total DOS is significantly low and the unique electronic state may correlate with the high antiferromagnetic stability [11]. Gradual increase of γ in M phase region would be due to the loss in antiferromagnetic stability.

In the P phase region, both γ and θ_D increase with decreasing In content. Although the variation of θ_D is similar to that observed in the M phase, the values do not coincide in the middle composition region. From the extrapolations in both the phases (the dotted lines for θ_D), it seems that θ_D changes discontinuously around x = 15, the difference corresponds to the change in θ_D during the martensitic phase transformation. Overall, θ_D in the M phase is larger than that in the P phase, in accordance

with the experimental fact that the volume of the M phase is more compressive than that of the P phase [27]. The variation of γ agrees well with the value obtained by first-principle density-functional calculations [10]. DOS in the P phase for the stoichiometric and off-stoichiometric compositions have been calculated, and γ values converted from total DOS are also plotted in Figure 5. DOS in the M phase was also calculated by applying the lattice distortion. The gradual increase of γ in the P phase is in accordance with that obtained by calculations. The theoretical calculations have shown that the minor peak corresponding to the Ni-3*d* e_g state appears at the energy level of -0.1 eV from E_F in the minority band for the off-stoichiometric composition, and the minority peak shifts closer to the E_F with increasing In content. Therefore, the shift in the minor peak will increase the total DOS because the DOS in the majority band is independent of the In content. Furthermore, the experimental value of γ at $x = 13$ is almost the same as the calculated one. Based on the extrapolations of the concentration dependence of γ in both the phases, a change in DOS is expected in the transformation. In other words, DOS is reduced when the P phase transforms to the M phase. This behavior has also been explained by the theoretical calculations that the minority-spin Ni-3*d* x^2–y^2 splits on introducing the lattice distortion and a pseudo-gap is formed at E_F [10]. The other calculation also suggested that the splitting of the Ni-3*d* e_g states around E_F plays an important role in occurrence of the martensitic transformation in the off-stoichiometric Ni-Mn-In alloy [28].

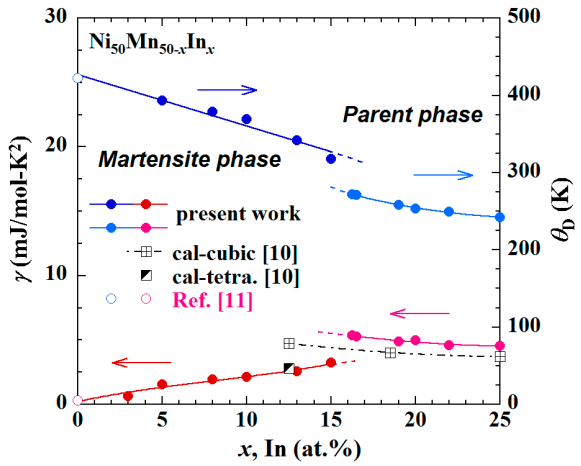

Figure 5. Concentration dependences of the electronic specific heat coefficient (γ) and the Debye temperature (θ_D) for $Ni_{50}Mn_{50-x}In_x$ alloys, along with the reported theoretically calculated values [10] and reported ones for $x = 0$ [11]. The blue and light blue circles are θ_D in M phase and P phase, respectively, and the red and pink circles are γ in M phase and P phase, respectively. The four lines are guide to the eye.

4. Conclusions

Specific heat measurements were performed at low-temperatures in $Ni_{50}Mn_{50-x}In_x$ alloys for $0 \leq x \leq 25$ to investigate the concentration dependences of electronic specific heat coefficient (γ) and the Debye temperature (θ_D) over a wide concentration region. In the martensite (M) phase ($x \leq 15$), θ_D decreases linearly and γ increases with increasing In content. The change in θ_D attributed to the substitution effect by the heavy element In. The increase in γ is attributed to the change in the density of states (DOS), and the clear pseudo-gap formed around the Fermi energy (E_F) may widen with the disappearance of the strong antiferromagnetism in $L1_0$-type NiMn equiatomic alloy, whereas the pseudo-gap is somewhat maintained within the M phase.

In the ferromagnetic parent (P) phase ($x \geq 16.2$), γ increases with decreasing In content. The change in DOS, in accordance with the first-principle density-functional calculation results reported earlier, is that the minor peak in the minority band shifts closer to E_F with decreasing

In content. From the extrapolations of the composition dependences of γ and θ_D from both the phase regions, these values should change discontinuously during the martensitic phase transformation. The value of θ_D in the M phase is larger than that in the P phase, in accordance with the fact that the volume of the M phase is more compressive than that of the P phase. It is suggested that the DOS in P phase decreases during martensitic phase transformation. This behavior is explained by the theoretical calculations that the Ni-3*d* e_g band splits in the M phase and the pseudo-gap is formed around the E_F.

Acknowledgments: The authors thank Emeritus Takeshi Kanomata in Tohoku-Gakuin University for his useful discussion. This study was supported by Grant-in-Aids from the Japanese Society for the Promotion of Science (JSPS), Ministry of Education, Culture, Sports, Science and Technology (MEXT), Japan. Parts of this study were done at the Center for Low Temperature Science, Institute for Materials Research, Tohoku University.

Author Contributions: Rie Y Umetsu and Ryosuke Kainuma conceived and designed the experiments; Rie Y Umetsu, Xiao Xu, and Wataru Ito performed the experiments; Rie Y Umetsu analyzed the data and wrote the paper; discussion was held among all of the authors, and the manuscript was finalized under their agreements.

Conflicts of Interest: The authors declare no conflict of interest.

References

1. Sutou, Y.; Imano, Y.; Koeda, N.; Omori, T.; Kainuma, R.; Ishida, K.; Oikawa, K. Magnetic and martensitic transformations of NiMn*X* (*X* = In, Sn, Sb) ferromagnetic shape memory alloys. *Appl. Phys. Lett.* **2004**, *85*, 4358–4360. [CrossRef]
2. Kainuma, R.; Imano, Y.; Ito, W.; Sutou, Y.; Morito, H.; Okamoto, S.; Kitakami, O.; Oikawa, K.; Fujita, A.; Kanomata, T.; et al. Magnetic-field-induced shape recovery by reverse phase transformation. *Nature* **2006**, *439*, 957–960. [CrossRef] [PubMed]
3. Kainuma, R.; Imano, Y.; Ito, W.; Morito, H.; Sutou, Y.; Oikawa, K.; Fujita, A.; Ishida, K.; Okamoto, S.; Kitakami, O.; et al. Metamagnetic shape memory effect in a Heusler-type $Ni_{43}Co_7Mn_{39}Sn_{11}$ polycrystalline alloy. *Appl. Phys. Lett.* **2006**, *88*, 192513. [CrossRef]
4. Krenke, T.; Duman, E.; Acet, M.; Wassermann, E.F.; Moya, X.; Mañosa, L.; Planes, A. Inverse magnetocaloric effect in ferromagnetic Ni–Mn–Sn alloys. *Nat. Mater.* **2005**, *4*, 450–454. [CrossRef] [PubMed]
5. Oikawa, K.; Ito, W.; Imano, Y.; Sutou, Y.; Kainuma, R.; Ishida, K.; Okamoto, S.; Kitakami, O.; Kanomata, T. Effect of magnetic field on martensitic transition of $Ni_{46}Mn_{41}In_{13}$ Heusler alloy. *Appl. Phys. Lett.* **2006**, *88*, 122507. [CrossRef]
6. Han, Z.D.; Wang, D.H.; Zhang, C.L.; Tang, S.L.; Gu, B.X.; Du, Y.W. Large magnetic entropy changes in the $Ni_{45.4}Mn_{41.5}In_{13.1}$ ferromagnetic shape memory alloy. *Appl. Phys. Lett.* **2006**, *89*, 182507. [CrossRef]
7. Koyama, K.; Okada, H.; Watanabe, K.; Kanomata, T.; Kainuma, R.; Ito, W.; Oikawa, K.; Ishida, K. Observation of large magnetoresistance of magnetic Heusler alloy $Ni_{50}Mn_{36}Sn_{14}$ in high magnetic fields. *Appl. Phys. Lett.* **2006**, *88*, 132505. [CrossRef]
8. Yu, S.Y.; Liu, Z.H.; Liu, G.D.; Chen, J.L.; Cao, Z.X.; Wu, G.H.; Zhang, B.; Zhang, X.X. Large magnetoresistance in single-crystalline $Ni_{50}Mn_{50-x}In_x$ alloys (x = 14–16) upon martensitic transformation. *Appl. Phys. Lett.* **2006**, *89*, 162503. [CrossRef]
9. Zhang, B.; Zhang, X.X.; Yu, S.Y.; Chen, J.L.; Cao, Z.X.; Wu, G.H. Giant magnetothermal conductivity in the Ni–Mn–In ferromagnetic shape memory alloys. *Appl. Phys. Lett.* **2007**, *91*, 012510. [CrossRef]
10. Zhu, S.; Ye, M.; Shirai, K.; Taniguchi, M.; Ueda, S.; Miura, Y.; Shirai, M.; Umetsu, R.Y.; Kainuma, R.; Kanomata, T.; et al. Drastic change in density of states upon martensitic phase transition for metamagnetic shape memory alloy $Ni_2Mn_{1+x}In_{1-x}$. *J. Phys. Condens. Matter* **2015**, *27*, 362201. [CrossRef] [PubMed]
11. Umetsu, R.Y.; Sakuma, A.; Fukamichi, K. Magnetic properties and electronic structures of $L1_0$-type MnTM (TM = Ir, Pt, Pd and Ni) alloy systems. *Met. Mater. Process.* **2003**, *15*, 67–94. [CrossRef]
12. Umetsu, R.Y.; Fukamichi, K.; Sakuma, A. Electrical and magnetic properties, and electronic structures of pseudo-gap-type antiferromagnetic $L1_0$-type MnPt Alloys. *Mater. Trans.* **2006**, *47*, 2–10. [CrossRef]
13. Umetsu, R.Y.; Fukamichi, K.; Sakuma, A. Effective exchange constant and electronic structure of pseudo-gap-type $L1_0$-MnPd Alloys. *J. Phys. Soc. Jpn.* **2006**, *75*, 104714. [CrossRef]

14. Ito, W.; Imano, Y.; Kainuma, R.; Sutou, Y.; Oikawa, K.; Ishida, K. Martensitic and magnetic transformation behaviors in Heusler-type NiMnIn and NiCoMnIn metamagnetic shape memory Alloys. *Metall. Mater. Trans. A* **2007**, *38*, 759–766. [CrossRef]
15. Pál, L.; Krén, E.; Kádár, G.; Szabó, P.; Tarnóczi, T. Magnetic structures and phase transformations in Mn-based CuAu-I type alloys. *J. Appl. Phys.* **1968**, *39*, 538–544. [CrossRef]
16. Aksoy, S.; Posth, O.; Acet, M.; Meckenstock, R.; Lindner, J.; Farle, M.; Wassermann, E.F. Ferromagnetic resonance in Ni-Mn based ferromagnetic Heusler alloys. *J. Phys. Conf. Ser.* **2010**, *200*, 092001. [CrossRef]
17. Priolkar, K.R. Role of local disorder in martensitic and magnetic interactions in Ni–Mn based ferromagnetic shape memory alloys. *Phys. Status Solidi B* **2014**, *251*, 2088–2096. [CrossRef]
18. Krenke, T.; Acet, M.; Wassermann, E.F.; Moya, X.; Mañosa, L.; Planes, A. Ferromagnetism in the austenitic and martensitic states of Ni-Mn-In alloys. *Phys. Rev. B* **2006**, *73*, 174413. [CrossRef]
19. Yan, H.; Zhang, Y.; Xu, N.; Senyshyn, A.; Brokmeier, H.G.; Esling, C.; Zhao, X.; Zuo, L. Crystal structure determination of incommensurate modulated martensite in Ni–Mn–In Heusler alloys. *Acta Mater.* **2015**, *88*, 375–388. [CrossRef]
20. Umetsu, R.Y.; Fujita, A.; Ito, W.; Kanomata, T.; Kainuma, R. Determination of the magnetic ground state in the martensite phase of Ni–Mn–*Z* (*Z* = In, Sn and Sb) off-stoichiometric Heusler alloys by nonlinear AC susceptibility. *J. Phys. Condens. Matter* **2011**, *23*, 326001. [CrossRef] [PubMed]
21. Khovaylo, V.V.; Kanomata, T.; Tanaka, T.; Nakashima, M.; Amako, Y.; Kainuma, R.; Umetsu, R.Y.; Morito, H.; Miki, H. Magnetic properties of $Ni_{50}Mn_{34.8}In_{15.2}$ probed by Mössbauer spectroscopy. *Phys. Rev. B* **2009**, *80*, 144409. [CrossRef]
22. Kanomata, T.; Yasuda, T.; Sasaki, S.; Nishihara, H.; Kainuma, R.; Ito, W.; Oikawa, K.; Ishida, K.; Neumann, K.-U.; Ziebeck, K.R.A. Magnetic properties on shape memory alloys $Ni_2Mn_{1+x}In_{1-x}$. *J. Magn. Magn. Mater.* **2009**, *321*, 773–776. [CrossRef]
23. Şaşıoğlu, E.; Sandratskii, L.M.; Bruno, P. First-principles calculation of the intersublattice exchange interactions and Curie temperatures of the full Heusler alloys Ni_2MnX (*X* = Ga, In, Sn, Sb). *Phys. Rev. B* **2004**, *70*, 024427. [CrossRef]
24. Umetsu, R.Y.; Kusakari, Y.; Kanomata, T.; Suga, K.; Sawai, Y.; Kindo, K.; Oikawa, K.; Kainuma, R.; Ishida, K. Metamagnetic behaviour under high magnetic fields in $Ni_{50}Mn_{50-X}In_X$ (*X* = 14.0 and 15.6) shape memory alloys. *J. Phys. Appl. Phys.* **2009**, *42*, 075003. [CrossRef]
25. Miyamoto, T.; Ito, W.; Umetsu, R.Y.; Kainuma, R.; Kanomata, T.; Ishida, K. Phase stability and magnetic properties of $Ni_{50}Mn_{50-x}In_x$ Heusler-type alloys. *Scr. Mater.* **2010**, *62*, 151–154. [CrossRef]
26. Gopal, E.S.R. *Specific Heats at Low Temperatures*; Plenum Press: New York, NY, USA, 1966.
27. Abematsu, K.; Umetsu, R.Y.; Kainuma, R.; Kanomata, T.; Watanabe, K.; Koyama, K. Structural and magnetic properties of magnetic shape memory alloy $Ni_{46}Mn_{41}In_{13}$ under magnetic fields. *Mater. Trans.* **2014**, *55*, 477–481. [CrossRef]
28. D'Souza, S.W.; Chakrabarti, A.; Barman, S.R. Magnetic interactions and electronic structure of Ni–Mn–In. *J. Electron Spectrosc. Relat. Phenom.* **2016**, *208*, 33–39. [CrossRef]